Journal of Plant Growth Regulation
https://doi.org/10.1007/s00344-023-11174-x

Spermidine Modulates Pollen Tube Growth by Affecting the Factors Involved in Pollen Tube Elongation

Çiğdem Tunur[1] · Aslıhan Çetinbaş-Genç[2]

Received: 15 May 2023 / Accepted: 4 November 2023

Abstract
Putrescine, spermine, and spermidine are among the most significant polyamines for plant growth and development, including pollen tube elongation. Although the effects of putrescine and spermine are well-known on tube elongation, little is known about the impact of spermidine. The aim of this study is to reveal how exogenic spermidine impinges positively and negatively on the factors involved in tube elongation such as actin cytoskeleton organization, calcium, pH and reactive oxygen species gradients, sucrose synthase enzyme activity, distribution of cell wall polysaccharide, tube nuclei movement. Treatment of 0.01 mM spermidine which showed a positive effect, increased actin dynamism, and, caused a decrease in the amount of cellulose in the tube apex by coordinating the sucrose synthase enzyme localization. These changes were reflected in the tube elongation velocities and oscillations as an increase, allowing the tubes to elongate faster. Treatment of 0.5 mM spermidine which showed a negative effect, caused changes in intracellular calcium, pH and reactive oxygen species gradients and these alterations reduced the dynamism of actin filaments. Decreased actin dynamism affected the localization of the sucrose synthase enzyme, inhibited the transport of newly synthesized wall materials to the tube apex and the transport of the generative nucleus to the tube apex. These changes were reflected in the tube elongation velocities and oscillations as a decrease, allowing the tubes to elongate slower. Results could be contributed to the explanation of the effect of spermidine in plant growth and development, including pollen tube elongation.

Keywords Exogenous treatment · Pollen tube elongation · Polyamines · Spermidine

Introduction

The pollen tube is a tubular extension of the pollen grain. Since sperm nuclei are immobile structures in angiosperms, they have to be transported to the embryo sac through pollen tubes meant for fertilization (Desnoyer et al. 2023). Therefore, from a reproductive biology perspective, pollen tube elongation is one of the most critical factors that affect the species' fertilization success. Various factors such as actin cytoskeleton organization, calcium (Ca^{+2}), pH and reactive oxygen species (ROS) gradients, sucrose synthase activity, distribution of cell wall polysaccharide, and the generative nucleus or sperm nuclei movement play a coordinated role in the elongation of the tube (Çetinbaş-Genç et al. 2022). So, these factors are considered so essential parameters for tube elongation.

Pollen tubes are elongated from the tip by the transportation of vesicles containing newly synthesized cell wall materials to the tube tip (Kapoor and Geitmann 2023). This transportation takes place via actin filaments, which are organized in different ways in various parts of the pollen tube. The long and parallel filaments in the shank region allow the vesicles to be transported over long distances, while the short, scattered, and highly dynamic filaments in the apex region allow the pollen tubes to fit quickly in the new growth conditions (Zhang et al. 2023). The filaments, organized in the fringe, get formed in a small area between the apex and the shank region, contribute to a tube elongation by providing the formation of new filaments yet preventing the passage

Handling Editor: Mohammad Irfan.

✉ Aslıhan Çetinbaş-Genç
aslihan.cetinbas@marmara.edu.tr

Çiğdem Tunur
cigdemtunur@marun.edu.tr

[1] Institute of Pure and Applied Sciences, Marmara University, 34722 Istanbul, Turkey

[2] Department of Biology, Faculty of Science, Marmara University, 34722 Istanbul, Turkey

Published online: 08 December 2023

of organelles to the tube tip (Lu et al. 2023). The transport of vesicles to the tube tip occurs as a result of the interaction between actin filaments with myosin, and the regulation of myosin activity depends on the intracellular Ca^{+2} gradient (Parrotta et al. 2022). So, it is significant to regulate myosin activity, especially at the tube tip, by the appropriate Ca^{+2} gradient for regular tube elongation (Qian and Xiang 2019). Besides, proper localization of ROS in the tubes regulates the tip-localized Ca^{+2} gradient via Ca^{+2} channels and controls the tube elongation by regulating the actin filaments and myosin activity, indirectly (Parrotta et al. 2019). In addition to that, the pH gradient in the pollen tube regulates the activity of actin-binding proteins (ABP) such as actin depolymerizing factor (ADF) and actin interacting protein (AIP). Since ADF and AIP are highly sensitive proteins to pH changes, alterations in pH gradient affect tube elongation by changing actin filament dynamics through modulation of ADF and AIP activities (Scholz et al. 2020). SUS, another crucial ABP for pollen tubes, contributes to tube elongation by converting sucrose to UDP-glucose, the precursor of the callose and cellulose which are the main cell wall components of the pollen tubes (Parrotta et al. 2022). The presence of callose and cellulose together with de-esterified pectin in the shank region mechanically strengthens the cell wall in this region. As a result of this increased structural stiffness, turgor pressure can elongate the pollen tube only from the tip region composed of esterified pectin and cellulose (Kapoor and Geitmann 2023). While all these factors ensure the tube elongation in a coordinated way, sperm nuclei are transported toward the tube tip by microtubules (Cai 2022).

Polyamines (PAs) are one of the far reaching regulator factors that is meant to be involved in pollen tube elongation (Aloisi et al. 2022). It is known that PA homeostasis in pollen grains has a great function on pollen tube elongation, as well as exogenous PAs can also significantly alter the tube elongation (Benko et al. 2020; Aloisi et al. 2022). PAs can also transform the activities of cytoskeletal elements in the pollen tube by binding into cytoskeletal monomers. Also, they can play a regulatory role in tube elongation as they can change the binding capacity of actin filaments to motor proteins such as myosin (Del Duca et al. 2009). Moreover, they can affect pollen tube elongation by regulating ion concentration in the pollen tubes, since they can regulate the ion transportation and activity of Ca^{+2} permeable channels. (Di Sandro et al. 2010; Wu et al. 2010). In addition, since PAs can quickly bind to pectic contents, they can regulate the organization of cell wall polysaccharides by binding to the apex. They can also organize the enzymatic activity of pectin methyl esterase, leading to a reduction of non-esterified pectin and thus causing softer cell wall formation (Charnay et al. 1992).

There are various studies on the effects of the most common PAs in plants, putrescine (Put) and spermine (Spm), on pollen tube elongation (Sorkheh et al. 2011, Do et al. 2019; Benko et al. 2020). However, little is known about the effects of another most common PA in plants, spermidine (Spd), on pollen tube elongation (Wu et al. 2010). Whereas, considering that most of the endogenic Spd are localized in the cell wall compartment, it is likely that exogenic Spd can change the distribution of cell wall components by interacting with different molecules (Del Duca et al. 2009). Since the distribution of the pollen tube's cell wall components is closely related to the actin cytoskeleton organization, Ca^{+2}, pH, and ROS gradient, it can be assumed that Spd may also be effective on these parameters. Although it has been reported that exogenic Spd treatments affect pollen tube elongation in various species such as *Malus domestica* (Del Duca et al. 1997), *Lycopersicon esculentum* (Song et al. 1999), *Prunus mume* (Wolukau et al. 2004), *Prunus dulcis* (Sorkheh et al. 2011) and *Camellia sinensis* (Çetinbaş-Genç et al. 2020a), there is limited information on how Spd affects the factors that work coordinately in pollen tube elongation. For instance; Wu et al. (2010) reported that exogenic Spd treatments might affect tube elongation by changing the Ca^{+2} gradient, hydrogen peroxide, and ROS production in pollen tubes of *Arabidopsis thaliana*, and by causing a change in cytosolic Ca^{+2} concentration in *Pyrus pyrofolia*'s pollen tubes. Whereas, there is no doubt that more information is needed on how exogenic Spd alter the factors that work coordinately in pollen tube elongation.

In this study, pollen grains from *Prunus domestica* were used in this study due to the facts that there is no previous study on this species on the subject, the species has economic importance, the species is a representative species for the Prunus genus, the species allows the collection of large amounts of pollen material easily, the species has pollen grains that are suitable for storage and germinate easily and quickly. *Prunus domestica*'s pollen grains were studied to reveal how exogenic Spd treatment impinges the factors involved in pollen tube elongation and to demonstrate how Spd-induced changes in these factors are reflected in pollen tube elongation. The effects of different spermidine concentrations on pollen germination and tube elongation were revealed in *Prunus mume* (Wolukau et al. 2004) and *Prunus dulcis* (Sorkheh et al., 2011), which are species close to *Prunus domestica*. However, in these studies, only pollen germination rates and tube lengths were used as evaluation criteria. However, unlike these studies, in the current study, Spd concentrations with the most negative and the most positive effects on tube elongation were determined using the germination rate and tube length parameters, and the consequences of these concentrations on the factors involved in pollen tube elongation were examined in details. It is thought that the results will contribute to the understanding of the cellular action mechanisms of Spd in pollen tubes, explaining more clearly the connections between the processes

and molecules involved in pollen tube elongation and, sighting the importance of the balance between them.

Material and Methods

Pollen Material

Pollen grains of *Prunus domestica* were harvested from plants grown on the Campus of Marmara University in May-April 2022. After dehydration overnight in a silica gel desiccator, they were stored at -20 °C until use. Pollen viability tested periodically during the all working progress.

In-vitro Pollen Germination and Tube Elongation

After being rehydrated for one hour in a humid chamber, pollen grains were allowed to germinate for 1 h in a Brewbaker and Kwack's medium with 12% sucrose (Brewbaker et al. 1963; Calic et al. 2013). The medium was supplemented with 0.01 mM, 0.025 mM, 0.05 mM, 0.1 mM, 0.25 mM, or 0.5 mM Spd for treatment groups and Spd-free medium was used to control. Pollen germination and tube elongation were examined under a light microscope and micrographs then were captured. Pollen grains with tubes longer than pollen diameter were considered as germinated. Germination rates were calculated by examining at least 1500 pollen grains for each group, using the 'Multi point' option of ImageJ software. Pollen tube lengths were calculated by delving into at least 1500 pollen tubes for each group, using the 'Segmented Line' option of Image J software.

Cumulative Stress Response Index (CSRI)

To identify the Spd treatment groups showing the most negative and most positive effects, the cumulative stress response index (CSRI) of each group was calculated according to the equation proposed by Dai et al. (1994). Germination rates (GR) and tube lengths (TL) of control (c) and treatment (t) groups were used to calculate CSRI values. The CSRI value of each group was calculated using the formula below.

$$\mathrm{CSRI} = \left(\frac{\mathrm{GRt} - \mathrm{GRc}}{\mathrm{GRc}} + \frac{\mathrm{TLt} - \mathrm{TLc}}{\mathrm{TLc}}\right) \times 100$$

The standard deviation (SD) of all obtained CSRI values was determined, and also the CSRI value of the treatment group that showed the minimum CSRI (mCSRI) value was noted. The evaluation was performed using the mCSRI value and the SD value as follows.

$$\begin{aligned}&\text{Intolerant} < \mathrm{mCSRI} + 1\ \mathrm{SD} < \text{Medium tolerant}\\ &< \mathrm{mCSRI} + 2\ \mathrm{SD} < \text{Tolerant} < \mathrm{mCSRI} + 3\ \mathrm{SD}\end{aligned}$$

As we aimed to reveal both negative and positive effects of Spd on pollen tube elongation, one treatment group showing the most negative and one treatment group showing the most positive effects were selected using the CSRI value, and further experiments were conducted in these groups.

Tube Growth Dynamics and Kymograph Analysis

In order to observe the effects of Spd treatments on the tube growth dynamics and oscillations, randomly selected 5 pollen grains' tube elongations were observed for each group. Tube elongations during the 1 h germination period were photographed every 5 min and tube lengths were calculated using the ImageJ software. The tube elongation velocity was calculated by dividing the determined tube elongation length every 5 min by 5. First, tube elongation velocities of the groups were compared between minutes, and then pollen tube elongation velocities of the groups per minute were compared among the groups. Afterward, in order to make a general evaluation, a pollen tube elongation velocity profile was created to show the elongation velocities of the groups every 5 min. To make kymograph analysis, 12 photos were taken for each pollen tube then converted into image series with the 'Image to Stack' plugin of the Fiji software. For each frame in the image series, the gray values in a specific area of interest were analyzed and the series were converted into kymograph profiles with the 'Multi Kymograph' plugin of the Fiji software.

Actin Filament Dynamics

Pollen tubes were fixed for 30 min by a fixation buffer (pH 6,9) containing 100 mM PIPES, 5 mM $MgSO_4$, 0.5 mM $CaCl_2$, 0.05% (v/v) Triton X-100, 1.5% (v/v) formaldehyde and 0.05% (v/v) glutaraldehyde. After washing with a washing buffer, which is formaldehyde- and glutaraldehyde-free version of the fixation buffer, tubes were incubated for 15 min in the washing buffer containing Alexa 488-phalloidin. After rewashing, actin organization was examined with a fluorescence microscope at 488–515 nm and micrographs were captured (Lovy-Wheeler et al. 2005). We look after it carefully in order to be capable of using both the same focal plane and the fluorescence settings for all groups. To get quantitative results, actin filament anisotropy values in the apex and shank regions were measured using "Fibril Tool" plugin of ImageJ software, in at least 20 pollen tubes with the equivalent length for each group (Boudaoud et al. 2014). Signals were reset against background noise. Anisotropy analysis was not performed in the sub-apex region because the actin fringe

is a very small region of the tube and it was very difficult to observe. The apex region was selected as a 10 µm segment from the tube tip and the shank region was selected as a 40 µm segment from the border of the apex region. According to the anisotropy analysis, 0 value represented high actin dynamism, while 1 value represented the least actin dynamism.

Ca^{+2}, pH and ROS Gradients

Pollen tubes were labeled with 5 µM Chlortetracycline hydrochloride (CTC) for Ca^{+2}, 5 µM 2′, 7′-bis-(2-Carboxyethyl)-5-(and-6)-carboxyfluorescein acetoxymethyl ester (BCECF-AM) for pH and 20 µM 2',7'-dichlorodihydrofluorescein diacetate (H_2DCFDA) for ROS. Ca^{+2}, pH, and ROS gradients within the tubes were examined with a fluorescence microscope at 515–536 nm, 440–490 nm, and 500–535 nm, respectively, and micrographs were captured within 5 min after the probes were added to the pollen tubes. In situ calibration of BCECF-AM was conducted according to Fricker et al. (1997). Carefully it was taken to be used for both same focal plane and fluorescence settings for all groups. For more efficient detailed analysis, micrographs were converted to 16 color scale using ImageJ. To get quantitative results, the normalized fluorescence intensities of probes in a 100 µm^2 area of the apical region were measured using the 'Rectangle Selection' option of ImageJ software, in at least 20 tubes with the equivalent length for each group. The normalized fluorescence intensities of probes were also measured inside the pollen tube along its growth axis, starting from the outermost tip to 50 µm backwards and using the 'Segmented Line' option of ImageJ with a selection width of about 4 µm. Signals were reset against background noise.

SUS Enzyme Localization

Pollen tubes were fixed for 30 min in a fixation buffer (pH 6.9) containing 50 mM PIPES, 0.5 mM $MgCl_2$, 1 mM EGTA, and 3% (*v*/*v*) formaldehyde. After washing with a washing buffer, which is a formaldehyde-free version of the fixation buffer, pollen tubes were incubated for 10 min in the washing buffer containing 1,5% cellulase and 1.5% pectinase. After rewashing, pollen tubes were incubated overnight in the washing buffer that contain 1:100 SUS primer antibody. After another rewash, pollen tubes were incubated for 45 min in the washing buffer containing 1:150 Alexa Goat anti-rabbit secondary antibody (Persia et al. 2008). After the last washing operation, sucrose synthase enzyme localization was examined with a fluorescence microscope at 488–515 nm and micrographs were captured. With a lot of care, both same focal plane and fluorescence settings were used for all groups. To get the quantitative results, the normalized fluorescence intensity of the SUS antibody in a 100 µm^2 area of the apical region was measured using the 'Rectangle Selection' option of Image J software, in at least 20 tubes with the equivalent length for each group. The normalized fluorescence intensity of the SUS antibody was also measured inside the pollen tube along its growth axis, starting from the outermost tip to 50 µm backwards using the 'Segmented Line' option of ImageJ with a selection width of about 4 µm. Signals were reset against background noise.

Callose, Cellulose and Pectin Distribution

Pollen tubes were stained with 0.1% Aniline blue for callose (Wang et al. 2003), 1% Calcofluor white for cellulose (Derksen et al. 2002), and 20 µM Propidium iodide for pectin (Rounds et al. 2011). Callose, cellulose, and pectin distributions were examined by a fluorescence microscope at 455–495 nm, 365–432 nm, and 482–608 nm, respectively, and micrographs were captured. Carefully, we use the same focal plane and the same fluorescence settings for all groups. To get the quantitative results, the normalized fluorescence intensities of stains in a 100 µm^2 area of the apical region were measured using the 'Rectangle Selection' option of Image J software, in at least 20 tubes with the equivalent length for each group. The normalized fluorescence intensities of stains were also measured on cell wall segments along its growth axis, starting from the outermost tip to 50 µm backwards using the 'Segmented Line' option of ImageJ with a selection width of about 2 µm. Signals were reset against the background noise.

Movement and Morphology of Generative Nucleus

Pollen tubes were labeled by 1 µg/ml 4′,6-diamidino-2-phenylindole (DAPI) (Covey et al. 2010). At least 50 pollen tubes for each group were examined with a fluorescence microscope at 358–461 nm and micrographs were captured. The micrographs of DAPI-labeled pollen tubes were also used to detect DNA damage in generative nuclei. With a lot of care, we use the same focal plane and the same fluorescence settings for all groups. Pollen tube lengths, and the distances of DAPI-labeled generative nuclei to the tube tip and also to the pollen grain were calculated using the 'Segmented Line' option of ImageJ software. The distances traveled by the generative nuclei in the pollen tube (%) were calculated by dividing the 100-fold distance of the generative nuclei to the pollen grain by the tube length. Also, the transport velocity (µm/min) of generative nuclei to the tube tip were calculated by dividing the distances of generative nuclei to the pollen grain by 60.

Statistical Analysis

All measurements were made in 3 repetitions. All measurement and calculation results were statistically compared by the ONE-WAY ANOVA ($p < 0.05$) test using the SPSS program.

Results

Pollen Germination Rate and Pollen Tube Length

In order to examine the effects of Spd treatment with different concentrations on pollen tube elongation, the fallout of Spd treatments on pollen germination and tube length were examined first and representative images are presented in Fig. 1a–g. No apparent morphological abnormality was observed in the pollen tubes of the control and treatment groups (Fig. 1h). The pollen germination rate was significantly decreased by 76.79% after 0.25 mM Spd and by 88.09% after 0.5 mM Spd treatment, compared to the control (Fig. 1i). There was no statistically prominent difference in pollen germination rate in other treatment groups, compared to the control. Compared to the control, pollen tube length increased statistically significantly by 14.02% after 0,01 mM Spd and by 8.12% after 0.05 mM Spd treatment. However, pollen tube length decreased significantly by 45.53% after 0.25 mM Spd and by 81.16% after 0.5 mM Spd treatment, compared to the control (Fig. 1j).

Evaluation of CSRI Values

As we aimed to reveal both negative and positive effects of Spd on pollen tube elongation, we calculated the CSRI values of the groups to determine the groups showing the most negative and positive consequences. An evaluation key was created based on the CSRI values. According to the evaluation key, it was determined that groups with a CSRI value below – 90.79 did not show tolerance to the specified Spd concentration, groups with a CSRI value between – 90.79 and – 12.31 showed medium tolerance to the specified Spd concentration, and also groups with a CSRI value

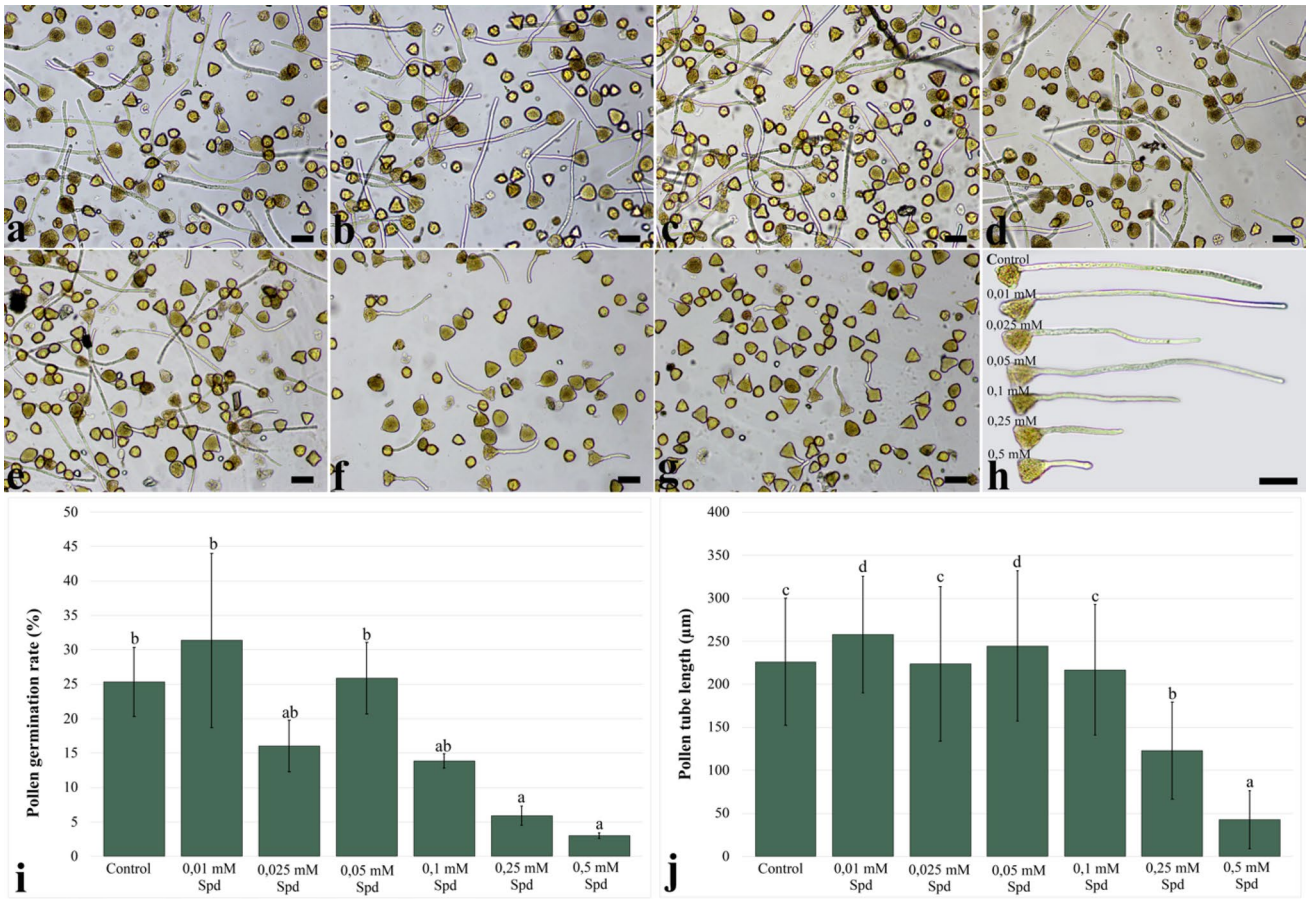

Fig. 1 Effect of Spd on pollen germination and tube elongation **a** Control. **b** 0,01 mM Spd. **c** 0,025 mM Spd. **d** 0,05 mM Spd. **e** 0,1 mM Spd. **f** 0,25 mM Spd. **g** 0,5 mM Spd. **h** Representative images of pollen tube. **i** Pollen germination rates (%). **j** Pollen tube lengths (µm). Bar: 50 µm. Vertical bars stand for standard errors among mean values at $p < 0.05$

between − 12.31 and 66.15 showed tolerance the specified Spd concentration. CSRI values revealed that the concentration with the best effect on tube elongation was 0.01 mM Spd and the concentration with the worst effect was 0.5 mM Spd (Table 1). Since it was targeted at clarifying both negative and positive activity of Spd concentrations on tube elongation, further experiments were performed in groups of 0.01 mM Spd, which showed the best effect, and 0.5 mM Spd, which showed the worst effect on tube elongation.

Tube Elongation Velocities and Kymograph Analysis

In order to observe the effects of Spd treatments on tube elongation velocities, tube elongation velocities of control, 0.01 mM Spd, and 0.5 mM Spd groups every 5 min for 1 h were calculated. First, the tube elongation velocities of each group were compared between minutes (5, 10, 15, 20, 25, 30, 35, 40, 45, 50, 55, 60). It was determined that the tube elongation velocities were maximum at 5th minutes for all groups. In the control and 0,5 mM Spd groups, tube elongation velocity was statistically significantly decreased at the 10th, 15th, 20th, 25th, 30th, 35th, 40th, 45th, 50th, 55th, and 60th minutes compared to the 5th minutes (Fig. 2a). After 0.01 mM Spd treatment, there was no statistically significant difference in pollen tube elongation velocities between minutes (Fig. 2a). Secondly, the tube elongation velocities of the groups at every 5 min were compared between the groups. Tube elongation velocities at the 5th, 10th, 15th, 20th, 25th, 30th, 35th, 40th, 45th, 50th, 55th, and 60th minutes did not show a statistically significant difference between the groups (Data not presented).

In order to make a general evaluation, a tube elongation velocity profile was created showing the tube elongation velocities of the groups in every 5 min for 1 h. According to this profile, the maximum elongation velocity values between the groups were observed in 4 time periods and the minimum elongation velocity values between the groups were observed in 2 time periods in the control group. After the treatment of 0.01 mM Spd, the maximum elongation velocity values between the groups were observed in 8 time periods, while the minimum elongation velocity values between the groups were not detected in any time period. Then, after the treatment of 0.5 mM Spd, the minimum elongation velocity values between the groups were observed in 8 time periods, while the maximum elongation velocity values between the groups were not detected in any time period (Fig. 2b).

In order to observe the effects of Spd treatments on the tube elongation oscillations, kymograph profiles of the groups were created. The linearity of the kymograph

Table 1 CSRI values

	0.01 mM	0.025 mM	0.05 mM	0.1 mM	0.25 mM	0.5 mM
CSRI	37.76	− 37.68	10.29	− 49.36	− 122.33	− 169.26
Evaluation	Tolerant	Medium tolerant	Tolerant	Medium tolerant	Intolerant	Intolerant
Evaluation key	Intolerant < − 90.79 < Medium tolerant < − 12.31 < Tolerant < 66.15					

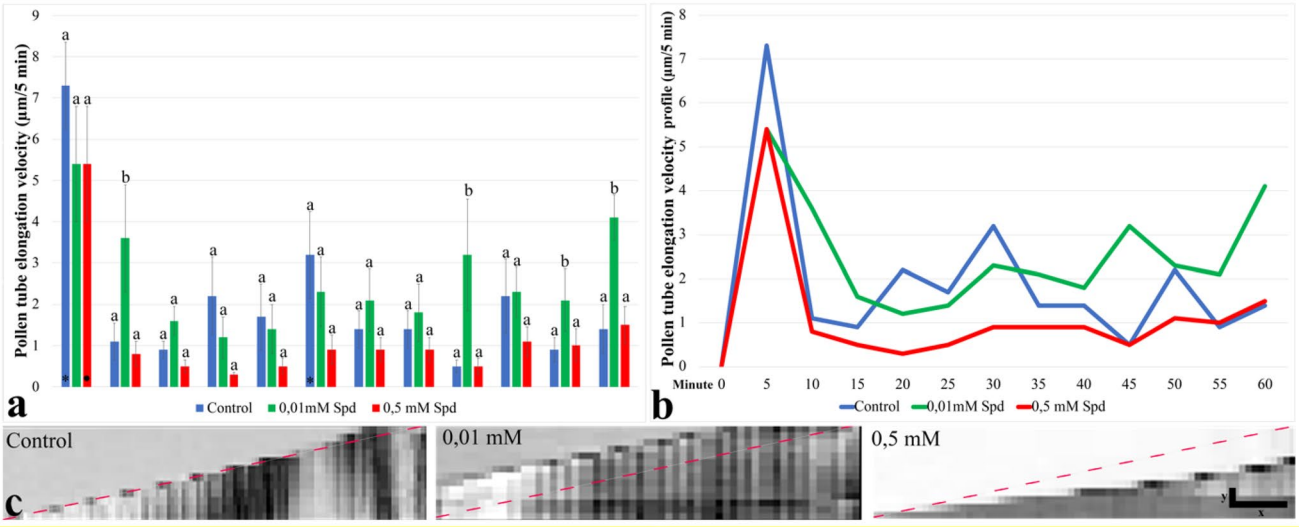

Fig. 2 Effect of Spd on tube elongation velocities and oscillations **a** Tube elongation velocity of control, 0,01 mM Spd and 0,5 mM Spd (µm/5 min). **b** Tube elongation velocity profile (µm/5 min). **c** Kymograph profiles. x bar: 5 min. Y bar: 20 µm. Vertical bars stand for standard errors among mean values at $p < 0.05$

profile in the control group revealed that the tube elongation oscillations were constant. After 0.01 mM Spd treatment, although the kymograph profile was linear from the 5th to the 60th minute, it was determined that the tube elongation oscillation increased compared to the control. After 0.5 mM Spd treatment, although the kymograph profile showed linearity up to about 5th minutes, it was determined that the growth oscillation was significantly reduced after the 5th minute compared to the control (Fig. 2c).

Organization of Actin Cytoskeleton

To observe the effects of Spd treatments on actin cytoskeleton organization in pollen tubes, the distribution of actin filaments in pollen tubes was examined. In control and after 0.01 mM Spd treatment, actin filaments were observed as long parallel bundles in the shank while they were observed as randomly arranged short filaments in the apex. After 0.5 mM Spd treatment, we have noticed that actin filaments were not fibrillar in the shank and were randomly packed in the apex (Fig. 3a). In order to make a quantitative evaluation, anisotropy values of actin filaments were analyzed in the shank and apex. According to the findings, actin filament anisotropy in the apex decreased statistically by 26.60% after 0.01 mM Spd treatment and increased significantly by 33.33% after 0.5 mM Spd treatment, compared to the control (Fig. 3b). Also, actin filament anisotropy in the shank increased significantly by 68.42% after 0.01 mM Spd and 168.42% after 0.5 mM Spd treatment, compared to the control (Fig. 3c).

Ca^{+2} Gradient

CTC probe signal was examined in pollen tubes to observe the effects of Spd treatments on intracellular Ca^{2+} gradient in pollen tubes. In control, while the Ca^{+2} signal was intense in the apex, it gradually decreased towards the shank and formed a gradient. After 0.01 mM Spd treatment, there was no relative difference in the Ca^{+2} signal and gradient in the pollen tubes compared to the control. After 0.5 mM Spd treatment, the Ca^{+2} signal in the tube apex and shank was relatively stronger than the control and also the gradient was shorter but distinct (Fig. 4a). In order to make a quantitative evaluation, the normalized fluorescence intensity of the CTC probe was measured in a 100 μm^2 area of the apical region. Despite the no statistically significant difference in the Ca^{+2} signal in the apex after 0.01 mM Spd treatment compared to the control, the signal was increased statistically by 52.66% compared to the control after 0.5 mM Spd treatment (Fig. 4b). For a more detailed evaluation, the normalized fluorescence intensity of the CTC probe was measured inside the pollen tube along its growth axis, starting from the outermost tip to 50 µm backward with a selection width of about 4 µm. According to the findings, although the distribution of the Ca^{+2} signal in the tube showed numerical differences between the groups, their gradient models showed similar trends. In all groups, the Ca^{2+} signal increased up to 2–4 µm and then decreased up to 50 µm. Although the Ca^{2+} signal distribution in the control and 0.01 mM Spd groups were in similar ranges, deviations occurred in the Ca^{+2} signal distribution in the tube after 0.5 mM Spd treatment. After 0.5 mM Spd treatment, although the Ca^{2+} signal was significantly higher between 0 and 7 µm than the other groups, it progressed in similar ranges with the other groups after about 7 µm (Fig. 4c).

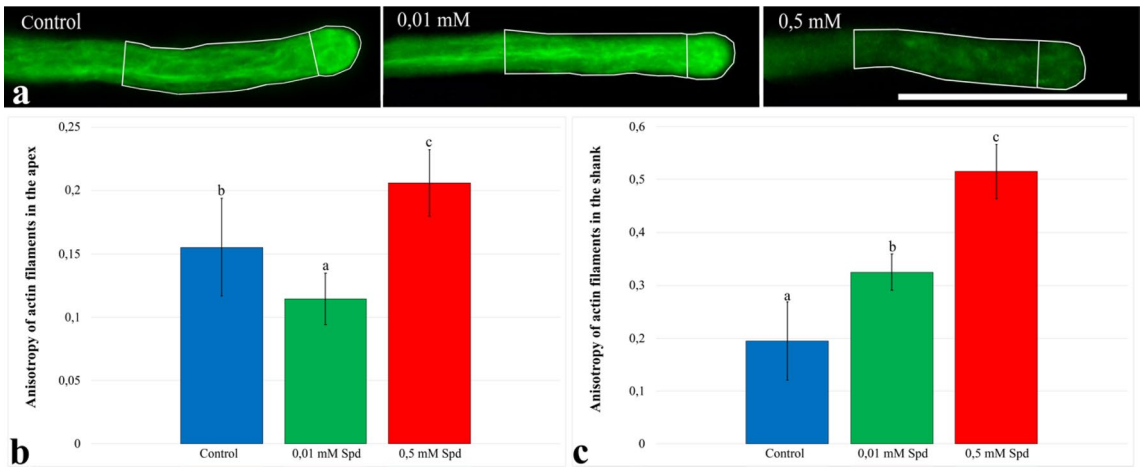

Fig. 3 Effect of Spd on organization of actin cytoskeleton **a** Representative images of actin filament distribution. **b** Anisotropy of actin filaments in the apex. **c** Anisotropy of actin filaments in the shank. Bar: 50 µm. Vertical bars stand for standard errors among mean values at $p < 0.05$

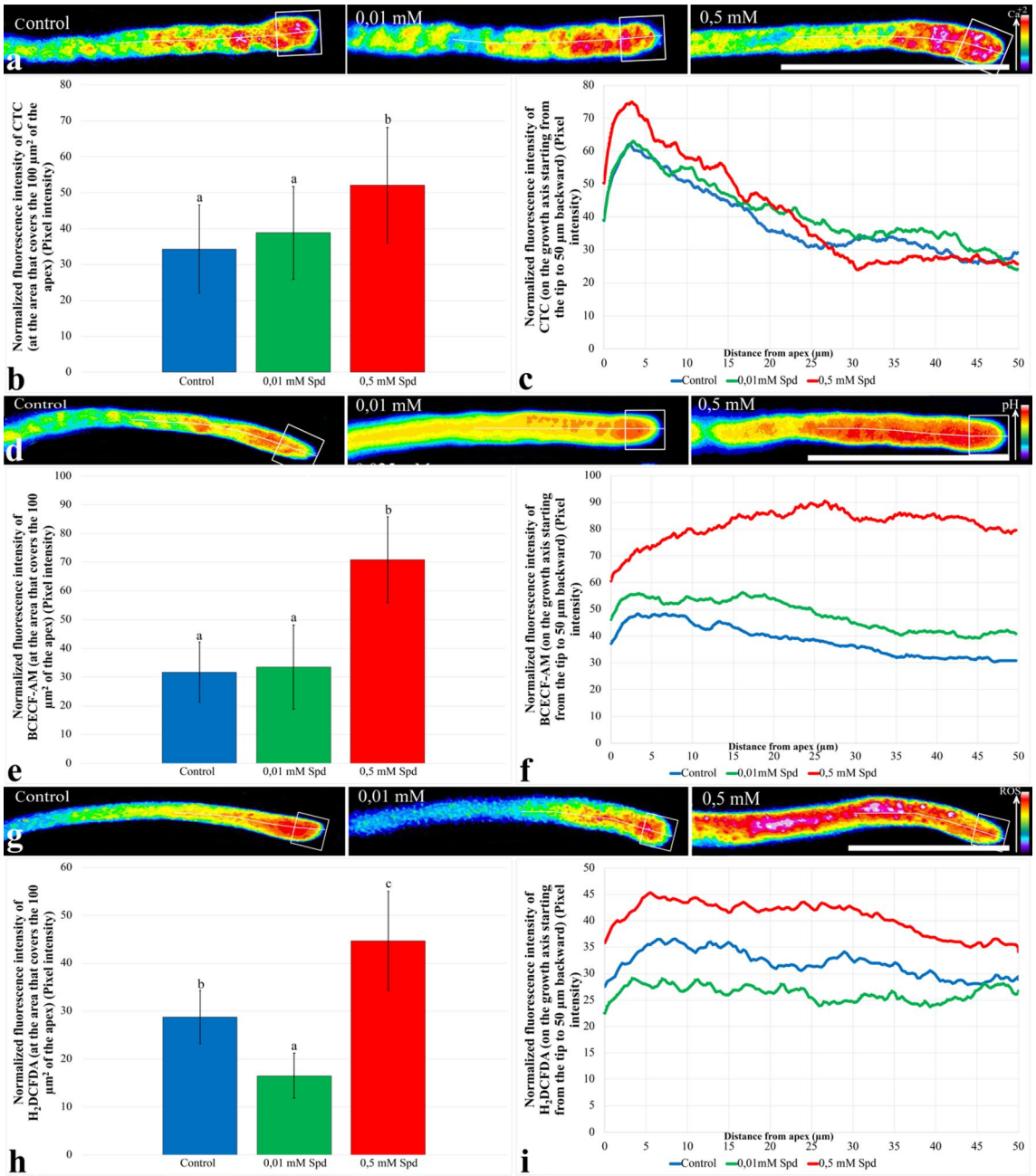

Fig. 4 Effect of Spd on organization of Ca^{+2}, pH and ROS gradient **a** Representative images of Ca^{+2} gradient. **b** Normalized fluorescence intensity of the CTC probe in a 100 μm^2 area of the apical region. **c** Normalized fluorescence intensity of the CTC probe on the growth axis starting from the tip to 50 µm backward. **d** Representative images of pH gradient. **e** Normalized fluorescence intensity of the BCECF-AM probe in a 100 μm^2 area of the apical region. **f** Normalized fluorescence intensity of the BCECF-AM probe on the growth axis starting from the tip to 50 µm backward. **g** Representative images of ROS gradient. **h** Normalized fluorescence intensity of the H_2DCFDA probe in a 100 μm^2 area of the apical region. **i** Normalized fluorescence intensity of the H_2DCFDA probe on the growth axis starting from the tip to 50 µm backward. Bar: 50 µm. Vertical bars stand for standard errors among mean values at $p < 0.05$

pH Gradient

BCECF-AM probe signal was examined in pollen tubes to observe the consequences of Spd treatments on intracellular pH gradient in pollen tubes. In control, while the pH signal was intense in the apex, it gradually decreased towards the shank and formed a gradient. After 0.01 mM Spd treatment, although a relative difference was not detected in the pH signal in the tube apex compared to the control, the pH signal was stronger than the control group in the shank. After

0.5 mM Spd, the pH signal throughout the tube was considerably higher than the control and the gradient began to deteriorate (Fig. 4d). In order to make a quantitative evaluation, the normalized fluorescence intensity of the BCECF-AM probe was measured in a 100 μm^2 area of the apical region. Although no significant difference was detected in the pH signal in the tube apex after 0.01 mM Spd treatment compared to the control, the signal increased statistically significantly by 122.90% after 0.5 mM Spd treatment, compared to the control (Fig. 4e). For a more detailed evaluation, the normalized fluorescence intensity of the BCECF-AM probe was measured inside the pollen tube along its growth axis, starting from the outermost tip to 50 µm backward with a selection width of about 4 µm. According to the findings, although the distribution of the pH signal in the tube showed numerical differences between the control and 0,01 mM Spd groups, their gradient models showed similar trends. In these groups, the pH signal has increased up to about 2–5 µm and then decreased gradually to up to 50 µm. After 0,5 mM Spd treatment, the pH signal increased up to 26 µm and then reduced up to 50 µm (Fig. 4f).

ROS Gradient

H_2DCFDA probe signal was examined in pollen tubes to observe the effects of Spd treatments on intracellular ROS gradient in pollen tubes. In control, while the pH signal was intense in the apex, it gradually decreased towards the shank and formed a gradient. After 0.01 mM Spd treatment, the ROS signal of both the apex and shank was weaker than the control. After 0.5 mM Spd treatment, the ROS signal in the apex and shank was higher than the control and the gradient began to deteriorate (Fig. 4g). In order to make a perceptible evaluation, the normalized fluorescence intensity of the H_2DCFDA probe was measured in a 100 μm^2 area of the apical region. According to the findings, after 0.01 mM Spd treatment, the ROS signal decreased statistically by 42.64% compared to the control, while the signal increased by 55.38% compared to the control, after 0.5 mM Spd treatment (Fig. 4h). For a more detailed evaluation, the normalized fluorescence intensity of the H_2DCFDA probe was measured inside the pollen tube along its growth axis, starting from the outermost tip to 50 µm backward with a selection width of about 4 µm. According to the findings, although the distribution of the ROS signal in the tube showed numerical differences between the groups, their gradient models showed similar trends. In control and 0.01 mM Spd groups, the ROS signal increased up to about 6 µm, then showed a relatively regular distribution down to 50 µm. However, after 0.5 mM Spd treatment, the ROS signal increased up to about 5–6 µm and then showed a relatively regular distribution with some reductions up to 50 µm (Fig. 4i).

Sucrose Synthase Enzyme Localization

SUS signal was examined in pollen tubes to observe the effects of Spd treatments on sucrose synthase enzyme localization in pollen tubes. In control, while the SUS signal was intense in the apex, it gradually decreased towards to the shank. No relative difference was detected in the SUS signal in pollen tubes after 0.01 mM Spd treatment, compared to the control. However, after 0.5 mM Spd treatment, the SUS signal in the apex was relatively stronger than the control and also, it was determined that SUS signal clusters were formed at the points close to the wall in the shank (Fig. 5a). In order to make a quantitative evaluation, the normalized fluorescence intensity of the SUS was measured in a 100 μm^2 area of the apical region. Although no important difference was detected in the SUS signal compared to the control after 0.01 mM Spd treatment, the SUS signal increased statistically by 72.15% compared to the control after 0.5 mM Spd treatment (Fig. 5b). For a more detailed evaluation, the normalized fluorescence intensity of the SUS was measured on cell wall segment of pollen tube along its growth axis, starting from the outermost tip to 50 µm backward with a selection width of about 2 µm. Although the SUS signal was in the same ranges in the control and 0,01 mM Spd groups between 0 and 5 µm, the signal was more intense after 0.5 mM Spd treatment. Although the SUS signal was almost equal in all groups between 5 and 15 µm, the signal was higher in the control and 0.5 mM Spd groups. After 15 µm, the SUS signal showed similar increasing trends in all groups including the control (Fig. 5c).

Callose, Cellulose and Pectin Distribution

Changes in the distribution of callose, cellulose and pectin were examined to observe the effects of Spd treatments on the pollen tube wall. According to the results of Aniline blue staining, it was determined that callose accumulated intensively on the pollen tube wall, excluding the apex, in the control group. Although there was no relative difference in callose accumulation in pollen tubes after 0.01 mM Spd treatment compared to control, dense callose accumulation in the tube apex after treatment of 0.5 mM Spd was quite remarkable (Fig. 5d) In order to make a quantitative evaluation, the normalized fluorescence intensity of the Aniline blue was measured in a 100 μm^2 area of the apical region. According to the findings, although no statistically significant difference could be detected in the callose deposition of tube apex after 0.01 mM Spd treatment compared to the control, the callose accumulation of tube apex increased statistically by 179.62% compared to the control after 0.5 mM Spd treatment (Fig. 5e). For a more detailed evaluation, the normalized fluorescence intensity of the Aniline blue was measured on cell wall segment of pollen tube along its

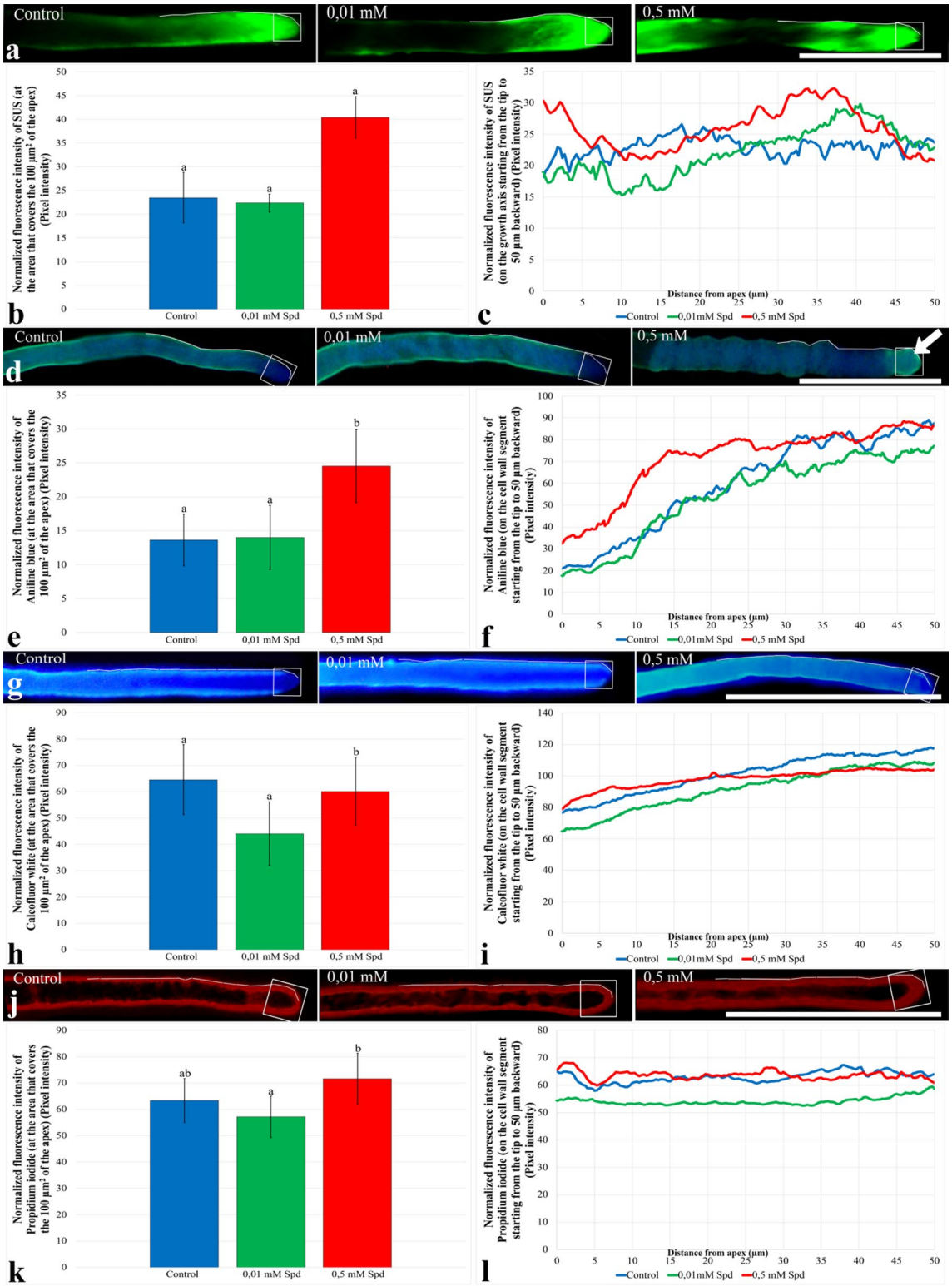

growth axis, starting from the outermost tip to 50 µm backward with a selection width of about 2 µm. According to the findings, it was determined that the distribution of callose in pollen tubes belonging to the control and 0.01 mM Spd groups increased regularly, showing similar trends from the tube apex to the shank. However, after 0.5 mM Spd treatment, callose accumulation between 0 and 30 µm was found to be higher than the other groups (Fig. 5f).

According to the results of Calcofluor white, it was determined that cellulose accumulated along the entire

◂**Fig. 5** Effect of Spd on the distribution of sucrose synthase enzyme and cell wall polysaccharides **a** Representative images of sucrose synthase enzyme distribution. **b** Normalized fluorescence intensity of the SUS antibody in a 100 μm^2 area of the apical region. **c** Normalized fluorescence intensity of the SUS antibody on the cell wall segment starting from the tip to 50 µm backward. **d** Representative images of callose distribution. **e** Normalized fluorescence intensity of the Aniline blue in a 100 μm^2 area of the apical region. **f** Normalized fluorescence intensity of the Aniline blue on the cell wall segment starting from the tip to 50 µm backward. **g** Representative images of cellulose distribution. **h** Normalized fluorescence intensity of the Calcofluor white in a 100 μm^2 area of the apical region. **i** Normalized fluorescence intensity of the Calcofluor white on the cell wall segment starting from the tip to 50 µm backward. **j** Representative images of pectin distribution. **k** Normalized fluorescence intensity of the Propidium iodide in a 100 μm^2 area of the apical region. **l** Normalized fluorescence intensity of the Propidium iodide on the cell wall segment starting from the tip to 50 µm backward. Bar: 50 µm. Vertical bars stand for standard errors among mean values at $p < 0.05$

tube wall, including the apex, in all groups (Fig. 5g). As a result, the normalized fluorescence intensity of the Calcofluor white was measured in a 100 μm^2 area of the apical region. According to the results, cellulose deposition was statistically significantly reduced by 31.80% compared to the control after 0.01 mM Spd treatment, while there was no statistical difference in cellulose deposition after 0.5 mM Spd treatment compared to the control (Fig. 5h). For a more detailed evaluation, the normalized fluorescence intensity of the Calcofluor white was measured on cell wall segment of pollen tube along its growth axis, starting from the outermost tip to 50 µm backward with a selection width of about 2 µm. According to the maintaining results, it was determined that the cellulose distribution in the pollen tubes of all groups increased regularly from the tube apex to the shank. Although the cellulose distribution showed numerical differences between these groups, the scatter plots showed similar trends except for some minor differences (Fig. 5i).

According to the results achieved of Propidium iodide, it was finalized that pectin accumulated along the entire tube wall, including the apex, in control group. There was no relative difference in pectin accumulation in pollen tubes after 0.01 mM and 0.5 mM Spd treatments compared to control (Fig. 5j). In order to make a quantitative evaluation, the normalized fluorescence intensity of the Propidium iodide was measured in a 100 μm^2 area of the apical region. As a result, 0.01 mM and 0.5 mM Spd treatments did not create a statistically huge difference in pectin distribution compared to the control (Fig. 5k). For a more detailed evaluation, the normalized fluorescence intensity of the Propidium iodide was measured on cell wall segment of pollen tube along its growth axis, starting from the outermost tip to 50 µm backward with a selection width of about 2 µm. According to the findings, it was determined that the pectin distributions of all groups were in the same ranges and showed similar trends (Fig. 5l).

Movement and Morphology of Generative Nucleus

In order to observe the effects of Spd treatments on the movement of generative nuclei to the tube tip, distances of the generative nuclei to the tube tip and the distances of the generative nuclei to the pollen grain were calculated in the pollen tubes stained with DAPI. Then, using these measurements, the distance traveled by the generative nuclei in the pollen tube (%) and transport velocity of generative nuclei to the tube tip (µm/min) were calculated. After 0,01 mM Spd treatment, there was no statistically significant difference in the distance of generative nuclei to the pollen grain compared to the control, but after 0.5 mM Spd treatment, it decreased significantly by 86.61% compared to the control (Fig. 6a) After 0.01 mM Spd treatment, there was no statistically significant difference in the distance of generative nuclei to the tube tip compared to the control, but after 0.5 mM Spd treatment, it decreased significantly by 85.71% compared to the control (Fig. 6b). After the treatments of 0.01 mM Spd and 0.5 mM Spd, there was no statistically significant difference compared to the control group in the distance travelled by the generative nuclei in the tube (Fig. 6c). After 0.01 mM Spd treatment, there was no statistically important difference in the transport velocity of the generative nuclei compared to the control, but after 0,5 mM Spd treatment, it was decreased significantly by 86.55% when compared to the control (Fig. 6d). No damage was detected in the generative nuclei in any group, including the control (Fig. 6e).

Discussion

Pollen germination rates and pollen tube lengths are the main parameters used to monitor pollen tube elongation, and different concentrations of different PAs are known to have different effects on pollen germination and tube elongation (Sorkheh et al. 2011). Song et al. (1999) investigated the effects of 0,005 mM, 0.005 mM and 0.5 mM Spd concentrations on the pollen grains of *Lycopersicum esculantum* and reported that only 0.05 mM Spd increased the pollen germination rate and tube length. Wu et al. (2010) reported that 0.1 mM and 1 mM Spd increased pollen tube length in *Pyrus pyrifolia*. In the study conducted with pollen grains of *Pyrus communis*, it was determined that Spd concentrations of 1 µM, 10 µM, 100 µM, 250 µM, 400 µM, 500 µM, 750 µM, 1 mM, and 2 mM reduced the length of the pollen tube (Aloisi et al. 2015). Benkő et al. (2020) reported that 10 µM and 50 µM Spd concentrations applied to pollen grains increased pollen germination and tube elongation in *Nicotiana tabacum.* These findings reveal that different doses of Spd may have different effects on pollen of different species. In this study, it was revealed that 0.01 mM and

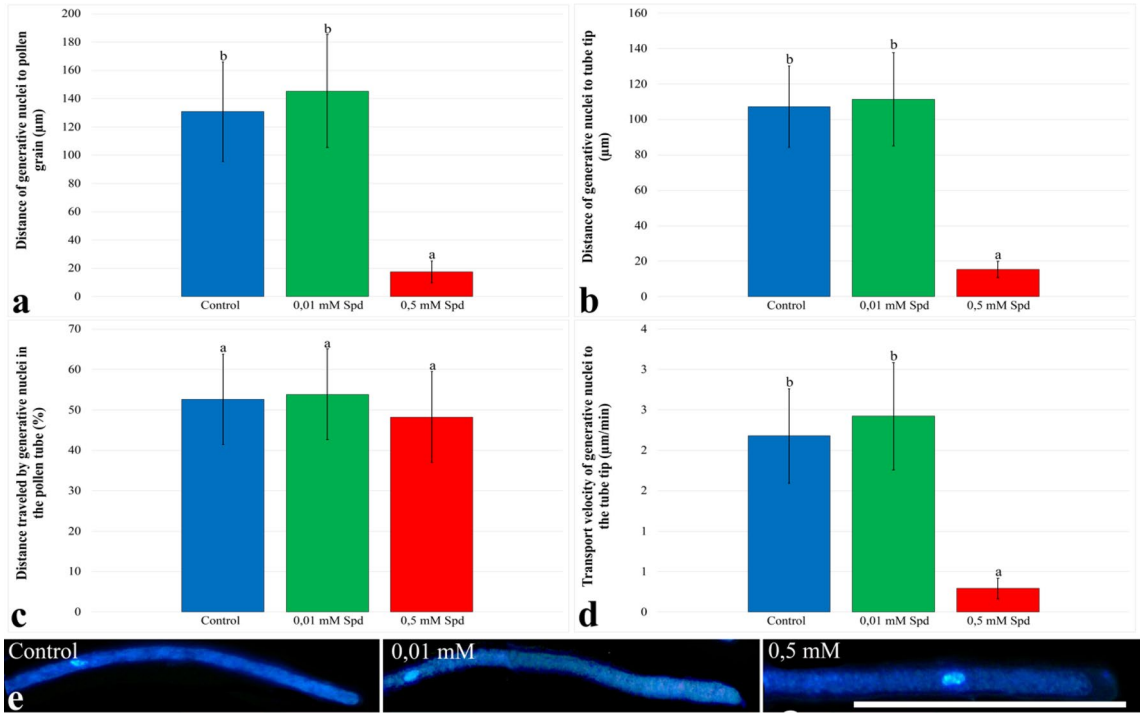

Fig. 6 Effect of Spd on the movement and morphology of generative nuclei **a** Distance of generative nuclei to pollen grain (µm). **b** Distance of generative nuclei to tube tip (µm). **c** Distance travelled by generative nuclei in the pollen tube (%). **d** Transport velocity of generative nuclei to the tube tip (µm/min). **e** Morphology of generative nuclei. Bar: 50 µm. Vertical bars stand for standard errors among mean values at $p < 0.05$

0.05 mM Spd concentrations increased the tube length, while 0.25 mM and 0.5 mM Spd concentrations decreased the tube length. Wolukau et al. (2004) have been studied with pollen grains of *Prunus mume*, a species close to *Prunus domestica*, and they determined that from 0.01 mM, 0.025 mM, 0.5 mM, to 2.5 mM Spd concentrations, only 2.5 mM Spd increased germination, and 0.025 mM and 0.25 mM Spd increased tube length. In addition, in a study conducted on *Prunus dulcis*, a species close to *Prunus domestica*, it has been reported that all concentrations except 2.5 mM Spd from 0.01 mM, 0.025 mM, 0.05 mM, 0.25 mM, 0.5 mM, and 2.5 mM Spd increased the pollen germination. In the same study, it was determined that 0.025 and 0.25 mM Spd concentrations increased the tube length (Sorkheh et al. 2011). When the findings of this study are compared with the findings of *Prunus mume* (Wolukau et al. 2004) and *Prunus dulcis* (Sorkheh et al. 2011), the observed differences support the idea that different doses of Spd may have different effects on pollen grains of different species.

Despite the fact that the most determining factors for monitoring pollen tube elongation are pollen germination and tube length, different internal or external parameters may have different effects on these factors. For instance, in this study, 0.01 mM Spd and 0.05 mM Spd treatments did not cause a statistically valuable change on pollen germination, yet aggrandized pollen tube lengths significantly compared to the control. Therefore, to examine the effects of any factor on pollen tube elongation, the results of pollen germination rate and tube length should be evaluated cumulatively (Dai et al. 1994). The CSRI assessment is often used to evaluate the effects of any stress factor on pollen tube elongation of different genotypes of a species (Liu et al. 2023). However, this evaluation can also be used to compare the effects of stress factors at different doses or application times on tube elongation of pollen belonging to a single genotype (Çetinbaş-Genç et al. 2022). Researchers used pollen germination rate and pollen tube lengths to determine CSRI values in their studies on *Olea europaea* and *Prunus dulcis* (Koubouris et al. 2009; Sorkheh et al. 2018). In addition, Koti et al. (2004) used pollen viability, pollen count and flower diameter as well as pollen germination rate and pollen tube lengths to evaluate the effects of CO_2, temperature and UV stress on pollen grains of *Glycine max*. Since it was aimed to clarify the negative and positive effects of Spd concentrations on tube elongation in this study, to detect the concentrations with the best and worst effect, pollen germination rate and pollen tube lengths were used to determine CSRI values. It was determined that 0.01 mM Spd treatment showed the best effect and 0.5 mM Spd showed the worst effect on tube elongation.

Researchers stated in their studies on *Lilium longiforum*, which is widely used as a model for in vitro pollen germination studies, that the pollen tube elongation velocity is slow in the first 1.5 h, but the elongation rate increases afterward (Cardenas et al. 2005). In this study, it was bent; that the pollen tube elongation velocity was maximum at the 5th minute for the control, 0.01 mM Spd and 0.5 mM Spd groups. Researchers have reported that the pollen tube elongation velocity in *Lilium longiforum* is 7.2–12 µm/min (Dong et al. 2012). Geitmann et al. (1996) reported that the pollen tube elongation velocity was 5 µm/min in *Nicotiana tabacum*. Pollen tube elongation velocity was found to be 1.2–12 µm/min in rbohh-1 rbohj-2 mutants and 3–6 µm/min in Col-0 mutant of *Arabidopsis thaliana* (Lassig et al. 2014). In this study, the elongation velocitiy of pollen tubes belonging to the control group was determined as 0.1–1.46 µm/min. The difference of these results to the literature can be explained by the differences in the examined species and germination times. In addition, according to the pollen tube elongation velocity profile obtained from this study, the maximum elongation velocity value among all groups was observed in a total of 8 time periods at 0.01 mM Spd concentration, which statistically increased the pollen tube length compared to the control, and this showed parallelism with the pollen tube length results. Likewise, the fact that 0.5 mM Spd concentration, which reduced the pollen tube length statistically significantly compared to the control group, showed a minimum elongation velocity in a total of 8 time periods, which showed parallelism with our pollen tube length results.

It has been determined that the pollen tube lengths of *Nicotiana tabacum* are reduced in pollen grains exposed to heat stress and this is reflected in tube elongation oscillations (Parrotta et al. 2016). In addition, it was also revealed that pollen tube lengths increased in pollen grains exposed to the cold stress of *Nicotiana tabacum*, and accordingly, pollen tube growth oscillations increased (Parrotta et al. 2019). Also, it was reported that pollen germination and tube elongation were decreased in AHA6, AHA8, and AHA9 mutants of *Arabidopsis thaliana*, and these effects were reflected in the kymograph profile in pollen tubes (Hoffman et al. 2020). It was stated that 400 µM Put applied to pollen grains of *Camellia sinensis* increased pollen tube length and pollen tube elongation oscillations, and 800 µM Put concentrations decreased pollen tube length and tube elongation oscillations (Çetinbaş-Genç 2020a). The kymograph profiles in this study showed parallelism with the pollen tube length results. It was determined that elongation oscillations increased after 0.01 mM Spd treatment, which increased the pollen tube length statistically significantly compared to the control group, and decreased after 0.5 mM Spd concentration, which significantly decreased the pollen tube length compared to the control group. These findings, which are in line with the literature, revealed that pollen tube length and pollen tube elongation release are closely related and that different Spd concentrations affect pollen tube lengths at different levels, causing different effects on pollen tube growth oscillations.

Researchers have reported that PAs can be covalently bound to actin monomers through the trans glutamine's enzyme, and they can change the binding capacity of actin filaments with motor proteins and may be a regulator of pollen tube elongation by modulating the activities of the actin cytoskeleton in the pollen tube (Aloisi et al. 2016). It has also been reported that high concentrations of PAs can block actin cytoskeletal dynamism (Del Duca et al. 2013). The outcomes of PAs on the actin cytoskeleton in pollen tubes have been previously studied by many researchers. Aloisi et al. (2017) determined that 100 µM Spm application reduced pollen tube length and pollen tube elongation velocity in *Pyrus communis* and reported that these changes were associated with changes in the actin cytoskeleton. It has been revealed that Put concentrations of 0.25 mM and above inhibit pollen tube elongation in *Corylus avellana* and this inhibition is associated with an increase in actin filament anisotropy (Çetinbaş-Genç et al. 2020b). It has also been reported that 400 µM Put treatment in *Camellia sinensis* increases pollen tube length by decreasing actin filament anisotropy in both apex and shank (Çetinbaş-Genç 2020a). In this study, the gaining dynamism of actin filaments in the apex after 0.01 mM Spd treatment is consistent with pollen tube length results. Because pollen tube lengths in this group also increased statistically significantly compared to the control group. In addition, after 0.5 mM Spd treatment, actin filaments in the apex lost their dynamism and pollen tube lengths in this group were statistically significantly decreased compared to the control. Therefore, the findings obtained from this study are compatible with the literature stating that the actin cytoskeleton plays a regulatory role in pollen tube elongation (Cai et al. 2015; Dong et al. 2012). Although the results of actin filament anisotropy in the apex were consistent with the pollen tube length findings, the decrease detected in actin filament dynamism in the shank after 0.01 mM Spd treatment did not show parallelism with the pollen tube length findings. However, the researchers stated that the actin filaments in the apex should be very dynamic to adapt to the changing growth conditions, and they emphasized that the actin filaments in this region are much more important for tube elongation than other regions (Cai et al. 2015). Therefore, it is thought that the consistency of the results in the apex with the pollen tube length may be sufficient to ignore results of shank in the treatment of 0.01 mM Spd.

Many researchers have associated the deterioration in the intracellular Ca^{+2} gradient with either the disruption of tube elongation or the inhibition of tube elongation (Monteiro et al. 2005; Winship et al. 2017). In regularly developing pollen tubes, the high Ca^{+2} concentration in the tube apex

decreases towards the shank (Konrad et al. 2011; Steinhorst and Kudla 2013). In this study, although the Ca^{+2} concentration in the tube showed numerical differences between the groups, the Ca^{+2} gradient was evident in the pollen tubes of all groups and was consistent with the literature. Polito (1983) stated that the pollen tube apex is rich in vesicles and that the Ca^{+2} concentration in this region will be an indicator of vesicle activity and thus tube elongation. In this study, it was determined that the Ca^{+2} concentration in the tube apex increased statistically significantly after only 0.5 mM Spd treatment compared to the control group. In addition, the sharp decrease in pollen tube length and the increase in actin anisotropy in the apex are also quite remarkable in this group. These findings suggested that after 0.5 mM Spd treatment, the high Ca^{+2} concentration in the tube apex and the deviations in the Ca^{+2} signal distribution throughout the tube disrupt the actin cytoskeleton dynamism and prevent the transport of vesicles to the tube tip, and thus this Spd concentration inhibits pollen tube elongation. Because it is known that the intense Ca^{+2} accumulation in the tube apex can trigger a series of dramatic effects such as depolymerization on the actin cytoskeleton (Aloisi et al. 2015).

Hepler (2016) reported that some stimuli may cause a change in membrane permeability by activating Ca^{+2} permeable channels in the plasma membrane or inner membranes. Ca^{+2} enters the pollen tube through Ca^{+2} channels in the apical plasma membrane and it is exported by Ca^{+2} pumps, thus maintaining Ca^{+2} homeostasis in the tube (Kroeger et al. 2008). PAs are known to regulate the elongation of pollen tubes by playing a role in modulating Ca^{+2} signaling (Pottosin and Shabala 2014). It has been demonstrated by various researchers that PAs can directly affect the activation of many ion channels, including Ca^{+2} channels (Abbasi et al. 2017; Kolupaev et al. 2022). It has been reported that the Ca^{+2} gradient localized in the tube apex in *Pyrus communis* changed after PA application (Aloisi et al. 2015). In addition, it has been deducted that the Ca^{+2} gradient in the tube apex changes after Spd treatment in *Camellia sinensis*, and it has been hypothesized that Spd is effective on Ca^{+2} channels in pollen tubes (Çetinbaş-Genç et al. 2020a). Therefore, in this study, it was thought that the high Ca^{+2} concentration in the tube apex observed after 0.5 mM Spd treatment may also be related to changing membrane permeability. However, there is no direct evidence in this study that 0.5 mM Spd treatments affects the Ca^{+2} channels in the tube apex and changes the membrane permeability.

Researchers stated that the apex of the pollen tubes is acidic and the acidity decreases towards the shank (Feijo et al. 1999). In this study, the pH gradient was evident in the 0.01 mM Spd group and was consistent with the literature. However, after 0.5 mM Spd treatment, the gradient started to deteriorate. Aloisi et al. (2017) found that pollen tube lengths decreased after 100 µM Spm treatment, and this decrease was accompanied by the change in the intracellular pH gradient in the pollen tube apex. It has also been shown that Spd applications at different concentrations cause pH changes in the pollen tubes of *Camellia sinensis* (Çetinbaş-Genç et al. 2020a). In this study, it was determined that intracellular pH increased in the tube apex in all groups except 0.01 mM Spd. The increase in actin anisotropy levels in the shank after all treatment groups and the minimum increase after 0.01 mM Spd treatment suggested that these findings were related to pH change. However, when the findings were compared with the results of actin filament anisotropy in the apex, no correlation was found between pH changes and actin anisotropy levels. However, considering that ADFs and AIPs are generally located in the actin fringe and take a more active role in the polymerization of long parallel actin bundles in the shank, it was thought that pH changes affect the organization of actin filaments in the shank rather than the apex (LovyWheeler et al. 2005). Besides, the highest pH concentration was observed in the 0.5 mM group throughout the tube, and it was thought that the increased acidity in the tube prevented the interaction of ADFs and AIPs with actin filaments, and inhibited the elongation of pollen tubes by preventing vesicle transport. Similarly, researchers stated that ADFs and AIPs can stop pollen tube growth by causing destabilization of actin filaments as a result of sharp changes in pH gradient (Lovy-Wheeler et al. 2005; Hepler et al. 2013).

Researchers have reported that there is a ROS gradient in the tube and the excessive ROS concentration in the apex of the tube decreases towards the shank (Wu et al. 2010). The intracellular ROS gradient observed in all groups in this study was consistent with the literature. Researchers have stated that ROS, especially localized in the tube apex, play a role in the organization of actin filaments by modulating the Ca^{+2} gradient in the tube apex (Wu et al. 2010). In this study, the changes observed in the accumulation of ROS in the tube apex after 0.01 mM Spd treatment were not reflected in the Ca^{+2} levels in the tube apex. However, the sharp increase in actin filament dynamism in this group, especially in the tube apex, suggested that ROS could affect actin cytoskeleton organization not only indirectly by modulating the Ca^{+2} gradient, but also directly, and could increase tube lengths. On the other hand, after 0.5 mM Spd treatment, ROS accumulation and Ca^{+2} concentration increased, and actin dynamism decreased. The decrease in tube length in this group is consistent with the literature stating that ROS may affect actin organization via Ca^{+2} and have a role on tube length (Potocky et al. 2012; Kaya et al. 2014). Also, similar to these findings, Benkő et al. (2020) stated that 10 µM Spd application in *Nicotiana tabacum* increased pollen tube lengths and decreased ROS levels in pollen tubes. In addition, it has been reported that pollen tube lengths decreased and ROS levels increased in *Arabidopsis thaliana* after 1 mM Spd

treatment (Wu et al. 2010). Comparably, it was determined that the pollen tube lengths of *Camellia sinensis* increased after 0.05 mM Spd treatment and this was accompanied by an increase in ROS accumulation in the tubes (Çetinbaş-Genç et al. 2020a).

Persia et al. (2008) have reported that they detected SUS signal in the apex of the normally elongating pollen tubes and near the wall of the shank of *Nicotiana tabacum*, but the signal was quite weak in the cytoplasm. In this study, it was determined that the SUS signal was intense in the tube apex and in the peripheral regions of the shank, but weak in the cytoplasm. Persia et al. (2008) reported that the intense SUS signal in the tube apex disappeared in the pollen tubes of *Nicotiana tabacum*, whose elongation was blocked by the application of brefeldin A. Parrotta et al. (2016) stated that the SUS signal was intense in the tube apex in elongating pollen tubes of *Nicotiana tabacum*, but the signal decreased towards the shank. In their study, the researchers have proclaimed that the SUS signal was preserved in the apical region in pollen tubes with reduced elongation and growth oscillations as a result of heat stress, but they saw irregular intense SUS signals in the cytoplasm in the shank. They associated this with changes in actin cytoskeleton organization as a result of heat stress. It was stated that the SUS signal in the pollen tubes of *Nicotiana tabacum*, whose growth was decreased down due to germination in a glycerol-based medium, increased in the shank by dispersing as dots in the cytoplasm. Researchers have associated these changes in SUS signal with glycerol-based distortions in pH and ROS gradients (Parrotta et al. 2018). Differences in sucrose synthase enzyme localization seen in pollen tubes of *Camellia sinensis*, whose growth has decreased due to exposure to high concentrations of Put, have also been associated with disruptions in actin cytoskeleton organization (Çetinbaş-Genç 2020a). In this study, it was thought that as a result of 0.5 mM Spd treatment, changes in intracellular Ca^{+2}, pH, and ROS gradients, as well as changes in actin anisotropy observed in both apex and shank, inhibited the elongation of pollen tubes by affecting the sucrose synthase enzyme localization in the tubes.

Parrotta et al. (2016) have stated that changes in actin cytoskeleton organization and sucrose synthase enzyme localization in pollen tubes may directly affect the structure of the pollen tube wall. In pollen grains of *Pyrus communis* exposed to 100 µM Spm, it has been reported that dense callose accumulation is observed in the tube apex, cellulose accumulation clusters are formed in the shank, and the pectin accumulation density in the wall changes (Aloisi et al. 2017). In their study, the researchers suggested that the intracellular pH gradient, which was disrupted as a result of the treatment of 100 µM Spm, modified the actin cytoskeleton and that this modification changed the transport of newly synthesized wall materials to the tube apex. Similarly, it has been reported that the changed actin skeletal organization in pollen tubes of *Camellia sinensis* were exposed to high concentrations of Put affects the localization of sucrose synthase enzyme and changes the tube distribution wall components (Çetinbaş-Genç 2020a). In this study, callose accumulation increased in the tubes after 0.5 mM Spd treatment. After the treatment of Spd at different concentrations, no acute change was observed in the pectin distribution in the tube wall. When all groups were evaluated, it was determined that actin filaments lost their dynamics in both apex and shank after only 0.5 mM Spd treatment. When the sucrose synthase enzyme localization results of this group were examined, it was determined that the SUS signal increased in the tube apex. When all these results were evaluated together, it was thought that 0.5 mM Spd caused an increase in the SUS signal in the tube apex by changing the actin organization both in the apex and shank, and the change in the sucrose synthase enzyme localization triggered the accumulation of callose in the tube apex. Similarly, it has been reported that changes in actin cytoskeleton organization due to heat stress in *Nicotiana tabacum* affect the distribution of sucrose synthase enzyme in the tubes and modify the distribution of tube wall components (Parrotta et al. 2016). Researchers have reported that disruptions in pH and ROS gradients in pollen tubes grown in glycerol-based medium of *Nicotiana tabacum* change the actin cytoskeleton organization, modify the localization of sucrose synthase enzyme in the tube, and affect the distribution of tube wall components in the tubes (Parrotta et al. 2018). Similarly, in this study, it was thought that the deteriorated intracellular Ca^{2+}, pH and ROS gradients after 0.5 mM Spd treatment changed actin cytoskeleton organization, sucrose synthase enzyme localization and wall structure, respectively. 0.1

Researchers have affirmed that the transport velocity of generative nuclei to the tube apex had not changed in the pollen tubes of *Nicotiana tabacum* whose growth decreased due to the heat stress (Parrotta et al. 2016). However, it has been reported that the transport velocity of generative nuclei to the apex of the tube decreases in the pollen tubes of *Nicotiana tabacum,* whose growth is reduced due to germination in a glycerol-based medium (Parrotta et al. 2018). In this study, the transport velocity of generative nuclei to the tube apex decreased only after treatment of 0.5 mM Spd. Researchers stated that microtubules play a role in the transport of generative and vegetative nuclei to the apex (Laitiainen et al. 2002). In light of this information, although it was thought that 0.5 mM Spd treatment might have changed the microtubule organization in pollen tubes, there is no direct evidence in this study. However, it is known that the transport of generative and vegetative nuclei to the pollen tube apex is coordinated by the synergistic relationship of microtubules with actin filaments (Poulter et al. 2008). In this study, actin filaments in both apex and shank regions

were affected by 0.5 mM Spd treatment, suggesting that these concentrations may have affected microtubule organization in the tubes either directly or indirectly through actin filaments. It has been reported that chromatin degradation in the generative nuclei is evident in pollen tubes of *Pyrus communis* treated with 100 µM Spm (Aloisi et al. 2015). In pollen tubes of *Camellia sinensis* exposed to high concentrations of Put, chromatin degradation was also detected in the generative nuclei (Çetinbaş-Genç 2020a). However, no damage was detected in the generative nuclei after Spd treatment in this study.

Conclusion

After the treatment of 0.01 mM Spd, 8 time periods with maximum elongation velocity, a sharp increase in tube elongation oscillations and an increase in actin filament dynamism in the apex were detected. The fact that there was no change in the intracellular Ca^{2+} and pH gradient in this group compared to the control, but sharp changes in the intracellular ROS gradient have revealed that the ROS accumulation seen in the tube apex after 0.01 mM Spd treatment increased the actin filament dynamism. It was interpreted that the increased actin dynamism caused a decrease in the amount of cellulose in the tube apex by coordinating the sucrose synthase enzyme localization, allowing the tubes to elongate faster. After 0.5 mM Spd treatment, 8 time periods with minimum elongation velocity and a sharp decrease in tube elongation oscillations were detected. It was determined that 0.5 mM Spd caused changes in intracellular Ca^{+2}, pH and ROS gradients in pollen tubes, and these changes reduced the dynamism of actin filaments in the apex and shank. It has been interpreted that the decreased actin dynamism inhibits the transport of newly synthesized wall materials to the tube apex and prevents the elongation of pollen tubes. In addition, it was determined that decreased actin dynamism affected the localization of the sucrose synthase enzyme, which converts sucrose to UDP-glucose, which is the precursor of cellulose and callose in the tube wall, and this effect was reflected in the tube wall as callose accumulation abnormalities. It has also been shown that 0.5 mM Spd inhibits the transport of the generative nucleus to the tube apex, but does not cause any damage to the nucleus. Results show how exogenic Spd treatment impinges the processes and molecules involved in pollen tube elongation in the most prominent examples. Obtained findings would contribute to the explanation of the cellular activity mechanism of Spd in both pollen tubes and other structures extending from the tip.

Acknowledgements Çiğdem Tunur would like to acknowledge The Scientific And Technological Research Council Of Türkiye (TÜBİTAK) for providing scholarship with 2210-A National Graduate Scholarship Program. This work was financially supported by the Marmara University Scientific Research Projects Commission (Project no: FYL-2022-10575).

Author Contributions ÇT and AÇG designed the work and performed the experiments. AÇG prepared the manuscript.

Declarations

Conflict of interest The authors declare that they have no conflict of interest.

References

Abbasi NA, Ali I, Hafiz IA, Khan AS (2017) Application of polyamines in horticulture: a review. Int J Biosci 10(5):319–342. https://doi.org/10.12692/ijb/10.5.319-342

Aloisi I, Cai G, Tumiatti V, Minarini A, Del Duca S (2015) Natural polyamines and synthetic analogs modify the growth and the morphology of *Pyrus communis* pollen tubes affecting ROS levels and causing cell death. Plant Sci 239:92–105. https://doi.org/10.1016/j.plantsci.2015.07.008

Aloisi I, Cai G, Serafini-Fracassini D, Del Duca S (2016) Polyamines in pollen: from microsporogenesis to fertilization. Front Plant Sci 7:155. https://doi.org/10.3389/fpls.2016.00155

Aloisi I, Cai G, Faleri C, Navazio L, Serafini-Fracassini D, Del Duca S (2017) Spermine regulates pollen tube growth by modulating Ca^{2+}-dependent actin organization and cell wall structure. Front Plant Sci 8:1701. https://doi.org/10.3389/fpls.2017.01701

Aloisi I, Piccini C, Cai G, Del Duca S (2022) Male fertility under environmental stress: Do polyamines act as pollen tube growth protectants? Int J Mol Sci 23(3):1874. https://doi.org/10.3390/ijms23031874

Benko P, Jee S, Kaszler N, Fehér A, Gémes K (2020) Polyamines treatment during pollen germination and pollen tube elongation in tobacco modulate reactive oxygen species and nitric oxide homeostasis. J Plant Physiol 244:153085. https://doi.org/10.1016/j.jplph.2019.153085

Boudaoud A, Burian A, Borowska-Wykręt D, Uyttewaal M, Wrzalik R, Kwiatkowska D, Hamant O (2014) FibrilTool, an ImageJ plug-in to quantify fibrillar structures in raw microscopy images. Nat Protoc 9:457–463. https://doi.org/10.1038/nprot.2014.024

Brewbaker JL, Kwack BH (1963) The essential role of calcium ion pollen germination and pollen tube growth. Am J Bot 50(9):859–865. https://doi.org/10.1002/j.1537-2197.1963.tb06564.x

Cai G (2022) The legacy of kinesins in the pollen tube 30 years later. Cytoskeleton 79(1–3):8–19. https://doi.org/10.1002/cm.21713

Cai G, Parrotta L, Cresti M (2015) Organelle trafficking, the cytoskeleton, and pollen tube growth. J Integr Plant Biol 57:63–78. https://doi.org/10.1111/jipb.12289

Calic D, Devrnja N, Kostic I, Kostic M (2013) Pollen morphology, viability, and germination of *Prunus domestica* cv. Požegača Sci Hortic 155:118–122. https://doi.org/10.1016/j.scienta.2013.03.017

Cardenas L, Lovy-Wheeler A, Wilsen KL, Hepler PK (2005) Actin polymerization promotes the reversal of streaming in the apex of pollen tubes. Cell Motil Cytoskelet 61(2):112–127. https://doi.org/10.1002/cm.20068

Çetinbaş-Genç A, Cai G, Del Duca S (2020a) Treatment with spermidine alleviates the effects of concomitantly applied cold stress by modulating Ca^{2+}, pH and ROS homeostasis, actin filament organization and cell wall deposition in pollen tubes of *Camellia sinensis*. Plant Physiol Biochem 156:578–590. https://doi.org/10.1016/j.plaphy.2020.10.008

Çetinbaş-Genç A, Cai G, Del Duca S, Vardar F, Ünal M (2020b) The effect of putrescine on pollen performance in hazelnut (*Corylus avellana* L.). Sci Hortic 261:108971. https://doi.org/10.1016/j.scienta.2019.108971

Çetinbaş-Genç A, Conti V, Cai G (2022) Let's shape again: the concerted molecular action that builds the pollen tube. Plant Reprod 35:77–103. https://doi.org/10.1007/s00497-022-00437-4

Charnay D, Nari J, Norat G (1992) Regulation of plant cell-wall pectin methyl esterase by polyamines-interactions with the effects of metal ions. Eur J Biochem 205(2):711–714. https://doi.org/10.1111/j.1432-1033.1992.tb16833.x

Covey PA, Subbaiah CC, Parsons RL, Pearce G, Lay FT, Anderson MA, Ryan CA, Bedinger PA (2010) A pollen-specific RALF from tomato that regulates pollen tube elongation. Plant Physiol 153(2):703–715. https://doi.org/10.1104/pp.110.155457

Dai Q, Peng S, Chavez AQ, Vergara BS (1994) Intraspecific response of 188 rice cultivars to enhanced UVB radiation. Environ Exp Bot 34(4):433–442. https://doi.org/10.1016/0098-8472(94)90026-4

Del Duca S, Bregoli AM, Bergamini C, Serafini-Fracassini D (1997) Transglutaminase-catalyzed modification of cytoskeletal proteins by polyamines during the germination of *Malus domestica* pollen. Sex Plant Reprod 10:89–95. https://doi.org/10.1007/s004970050072

Del Duca S, Serafini-Fracassini D, Bonner P, Cresti M, Cai G (2009) Effects of post-translational modifications catalysed by pollen transglutaminase on the functional properties of microtubules and actin filaments. Biochem J 418(3):651–664. https://doi.org/10.1042/BJ20081781

Del Duca S, Faleri C, Iorio RA, Cresti M, Serafini-Fracassini D, Cai G (2013) Distribution of transglutaminase in pear pollen tubes in relation to cytoskeleton and membrane dynamics. Plant Physiol 161(4):1706–1721. https://doi.org/10.1104/pp.112.212225

Derksen J, Knuiman B, Hoedemaekers K, Guyon A, Bonhomme S, Pierson ES (2002) Growth and cellular organization of Arabidopsis pollen tubes in vitro. Sex Plant Reprod 15:133–139. https://doi.org/10.1007/s00497-002-0149-1

Desnoyer NJ, Grossniklaus U (2023) Live imaging of Arabidopsis pollen tube reception and double fertilization using the semi-in vitro cum septum method. J vis Exp 192:e65156. https://doi.org/10.3791/65156

Di Sandro A, Del Duca S, Verderio E, Hargreaves AJ, Scarpellini A, Cai G, Cresti M, Faleri C, Iorio RA, Hirose S, Furutani Y, Coutts IGC, Griffin M, Bonner PLR, Serafini-Fracassini D (2010) An extracellular transglutaminase is required for apple pollen tube growth. Biochem J 429(2):261–271. https://doi.org/10.1042/BJ20100291

Do THT, Choi H, Palmgren M, Martinoia E, Hwang JU, Lee Y (2019) Arabidopsis ABCG28 is required for the apical accumulation of reactive oxygen species in growing pollen tubes. Proc Natl Acad Sci 116(25):12540–12549. https://doi.org/10.1073/pnas.1902010116

Dong H, Pei W, Haiyun R (2012) Actin fringe is correlated with tip growth velocity of pollen tubes. Mol Plant 5:1160–1162. https://doi.org/10.1093/mp/sss073

Feijó JA, Sainhas J, Hackett GR, Kunkel JG, Hepler PK (1999) Growing pollen tubes possess a constitutive alkaline band in the clear zone and a growth-dependent acidic tip. J Cell Biol 144(3):483–496. https://doi.org/10.1083/jcb.144.3.483

Fricker MD, White NS, Obermeyer G (1997) pH gradients are not associated with tip growth in pollen tubes of *Lilium longiflorum*. J Cell Sci 110(15):1729–1740. https://doi.org/10.1242/jcs.110.15.1729

Geitmann A, Li YQ, Cresti M (1996) The role of the cytoskeleton and dictyosome activity in the pulsatory growth of Nicotiana tabacum and *Petunia hybrida* pollen tubes. Plant Biol 109(2):102–109. https://doi.org/10.1111/j.1438-8677.1996.tb00549.x

Hepler PK (2016) The cytoskeleton and its regulation by calcium and protons. Plant Physiol 170(1):3–22. https://doi.org/10.1104/pp.15.01506

Hepler PK, Rounds CM, Winship LJ (2013) Control of cell wall extensibility during pollen tube growth. Mol Plant 6(4):998–1017. https://doi.org/10.1093/mp/sst103

Hoffmann RD, Portes MT, Olsen LI, Damineli DSC, Hayashi M, Nunes CO, Pedersen JT, Lima PT, Campos C, Feijo JA, Palmgren M (2020) Plasma membrane H^+-ATPases sustain pollen tube growth and fertilization. Nat Commun 11:2395. https://doi.org/10.1038/s41467-020-16253-1

Kapoor K, Geitmann A (2023) Pollen tube invasive growth is promoted by callose. Plant Reprod. https://doi.org/10.1007/s00497-023-00458-7

Kaya H, Nakajima R, Iwano M, Kanaoka MM, Kimura S, Takeda S, Kawarazak T, Senzaki E, Hamamura Y, Higashiyama T, Takayama S, Abe M, Kuchitsu K (2014) Ca^{2+}-activated reactive oxygen species production by Arabidopsis RbohH and RbohJ is essential for proper pollen tube tip growth. Plant Cell 26(3):1069–1080. https://doi.org/10.1105/tpc.113.120642

Kolupaev YE, Kokorev AI, Dmitriev AP (2022) Polyamines: involvement in cellular signaling and plant adaptation to the effect of abiotic stressors. Cytol Genet 56(2):148–163. https://doi.org/10.3103/S0095452722020062

Konrad KR, Wudick MM, Feijo JA (2011) Calcium regulation of tip growth: new genes for old mechanisms. Curr Opin Plant Biol 14(6):721–730. https://doi.org/10.1016/j.pbi.2011.09.005

Koti S, Reddy KR, Kakani VG, Zhao D, Reddy VR (2004) Soybean (*Glycine max*) pollen germination characteristics, flower and pollen morphology in response to enhanced ultraviolet-B radiation. Ann Bot 94(6):855–864. https://doi.org/10.1093/aob/mch212

Koubouris GC, Metzidakis IT, Vasilakakis MD (2009) Impact of temperature on olive (*Olea europaea* L.) pollen performance in relation to relative humidity and genotype. Environ Exp Bot 67(1):209–214. https://doi.org/10.1016/j.envexpbot.2009.06.002

Kroeger JH, Geitmann A, Grant M (2008) Model for calcium dependent oscillatory growth in pollen tubes. J Theor Biol 253(2):363–374. https://doi.org/10.1016/j.jtbi.2008.02.042

Laitiainen E, Nieminen KM, Vihinen H, Raudaskoski M (2002) Movement of generative cell and vegetative nucleus in tobacco pollen tubes is dependent on microtubule cytoskeleton but independent of synthesis of callose plugs. Sex Plant Reprod 15:195–204. https://doi.org/10.1007/s00497-002-0155-3

Lassig R, Gutermuth T, Bey TD, Konrad KR, Romeis T (2014) Pollen tube NAD(P)H oxidases act as a speed control to dampen growth rate oscillations during polarized cell growth. Plant J 78:94–106. https://doi.org/10.1111/tpj.12452

Liu X, Xiao Y, Zi J, Yan J, Li C, Du C, Wan J, Wu H, Zheng B, Wang S, Liang Q (2023) Differential effects of low and high temperature stress on pollen germination and tube length of mango (*Mangifera indica* L.) genotypes. Sci Rep 13(1):1–14. https://doi.org/10.1038/s41598-023-27917-5

Lovy-Wheeler A, Wilsen KL, Baskin TI, Hepler PK (2005) Enhanced fixation reveals the apical cortical fringe of actin filaments as a consistent feature of the pollen tube. Planta 221:95–104. https://doi.org/10.1007/s00425-004-1423-2

Lu Q, Liu X, Qu X, Huang S (2023) Visualization and quantification of the dynamics of actin filaments in Arabidopsis pollen tubes. In: Hussey PJ, Wang P (eds) The plant cytoskeleton. Methods in molecular biology. Humana, New York, pp 285–295

Monteiro D, Liu Q, Lisboa S, Scherer GEF, Quader H, Malho R (2005) Phosphoinositides and phosphatidic acid regulate pollen tube growth and reorietation through modulation of (Ca^{2+})C and membrane secretion. J Exp Bot 56(416):1665–1674. https://doi.org/10.1093/jxb/eri163

Parrotta L, Faleri C, Cresti M, Cai G (2016) Heat stress affects the cytoskeleton and the delivery of sucrose synthase in tobacco pollen tubes. Planta 243:43–63. https://doi.org/10.1007/s00425-015-2394-1

Parrotta L, Faleri C, Del Duca S, Cai G (2018) Depletion of sucrose induces changes in the tip growth mechanism of tobacco pollen tubes. Ann Bot 122(1):23–43. https://doi.org/10.1093/aob/mcy043

Parrotta L, Faleri C, Guerriero G, Cai G (2019) Cold stress affects cell wall deposition and growth pattern in tobacco pollen tubes. Plant Sci 283:329–342. https://doi.org/10.1016/j.plantsci.2019.03.010

Parrotta L, Faleri C, Del Casino C, Mareri L, Aloisi I, Guerriero G, Hausman JF, Del Duca S, Cai G (2022) Biochemical and cytological interactions between callose synthase and microtubules in the tobacco pollen tube. Plant Cell Rep 41:1301–1318. https://doi.org/10.1007/s00299-022-02860-3

Persia D, Cai G, Del Casino C, Faleri C, Willemse MT, Cresti M (2008) Sucrose synthase is associated with the cell wall of tobacco pollen tubes. Plant Physiol 147:1603–1618. https://doi.org/10.1104/pp.108.115956

Polito VS (1983) Membrane-associated calcium during pollen grain germination: a microfluorometric analysis. Protoplasma 117:226–232. https://doi.org/10.1007/BF01281826

Potocky M, Pejchar P, Gutkowska M, Jimenez-Quesada MJ, Potocka A, de Dios AJ, Kost B, Zarsk V (2012) NADPH oxidase activity in pollen tubes is affected by calcium ions, signaling phospholipids and Rac/Rop GTPases. J Plant Physiol 169(16):1654–1663. https://doi.org/10.1016/j.jplph.2012.05.014

Pottosin I, Shabala S (2014) Polyamines control of cation transport across plant membranes: implications for ion homeostasis and abiotic stress signaling. Front Plant Sci 5:154. https://doi.org/10.3389/fpls.2014.00154

Poulter NS, Vatovec S, Franklin-Tong VE (2008) Microtubules are a target for self-incompatibility signaling in Papaver pollen. Plant Physiol 146(3):1358–1367. https://doi.org/10.1104/pp.107.107052

Qian D, Xiang Y (2019) Actin cytoskeleton as actor in upstream and downstream of calcium signaling in plant cells. Int J Mol Sci 20(6):1403. https://doi.org/10.3390/ijms20061403

Rounds CM, Lubeck E, Hepler PK, Winship LJ (2011) Propidium iodide competes with Ca^{2+} to label pectin in pollen tubes and Arabidopsis root hairs. Plant Physiol 157(1):175–187. https://doi.org/10.1104/pp.111.182196

Scholz P, Anstatt J, Krawczyk HE, Ischebeck T (2020) Signaling pinpointed to the tip: the complex regulatory network that allows pollen tube growth. Plants 9(9):1098. https://doi.org/10.3390/plants9091098

Song J, Nada K, Tachibana S (1999) Ameliorative effect of polyamines on the high temperature inhibition of in vitro pollen germination in tomato (*Lycopersicum esculentum* Mill.). Sci Hortic 80(3–4):203–212. https://doi.org/10.1016/S0304-4238(98)00254-4

Sorkheh K, Azimkhani R, Mehri N, Chaleshtori MH, Halasz J, Ercisli S, Koubouris GC (2018) Interactive effects of temperature and genotype on almond (*Prunus dulcis* L.) pollen germination and tube length. Sci Hortic 227:162–168. https://doi.org/10.1016/j.scienta.2017.09.037

Sorkheh K, Shiran B, Rouhi V, Khodambashi M, Wolukau JN, Ercisli S (2011) Response of in vitro pollen germination and pollen tube growth of almond (*Prunus dulcis* Mill.) to temperature, polyamines and polyamine synthesis inhibitor. Biochem Syst Ecol 39(4-6):749–757. https://doi.org/10.1016/j.bse.2011.06.015

Steinhorst L, Kudla J (2013) Calcium: a central regulator of pollen germination and tube growth. Biochim Biophys Acta BBA Mol Cell Res 1833:1573–1581. https://doi.org/10.1016/j.bbamcr.2012.10.009

Wang Q, Lu L, Wu X, Li Y, Lin J (2003) Boron influences pollen germination and pollen tube growth in *Picea meyeri*. Tree Physiol 23:345–351. https://doi.org/10.1093/treephys/23.5.345

Winship L, Rounds C, Hepler P (2017) Perturbation analysis of calcium, alkalinity and secretion during growth of Lily pollen tubes. Plants 6:3. https://doi.org/10.3390/plants6010003

Wolukau JN, Zhang S, Xu G, Chen D (2004) The effect of temperature, polyamines and polyamine synthesis inhibitor on in vitro pollen germination and pollen tube growth of *Prunus mume*. Sci Hortic 99(3–4):289–299. https://doi.org/10.1016/S0304-4238(03)00112-2

Wu J, Shang Z, Wu J, Jiang X, Moschou PN, Sun W, Roubelakis-Angelakis KA, Zhang S (2010) Spermidine oxidase-derived H_2O_2 regulates pollen plasma membrane hyperpolarization-activated Ca^{2+}-permeable channels and pollen tube growth. Plant J 63(6):1042–1053. https://doi.org/10.1111/j.1365-313X.2010.04301.x

Zhang R, Xu Y, Yi R, Shen J, Huang S (2023) Actin cytoskeleton in the control of vesicle transport, cytoplasmic organization and pollen tube tip growth. Plant Physiol 00:1–17. https://doi.org/10.1093/plphys/kiad203